Thermochimica Acta, 79 (1984) 69–81
Elsevier Science Publishers B.V., Amsterdam – Printed in The Netherlands

TG STUDY ON THE REACTION OF γ-Al_2O_3 BY CCl_4. PART I. KINETIC MODEL FOR THE CHLORINATION PROCESS

I.S. PAP, I. BERTÓTI and GY. MINK

Research Laboratory for Inorganic Chemistry of the Hungarian Academy of Sciences, P.O.B. 112, Pf. 132, H-1502 Budapest (Hungary)

(Received 19 March 1984)

ABSTRACT

Thermogravimetric (TG) measurements were carried out to study the chlorination of γ-alumina by gaseous CCl_4 in the temperature range 650–1123 K at 10^2–10^4 Pa CCl_4 partial pressure. Experimental results indicate that the reaction involves two main steps: the substitution of oxygen atoms on the surface by chlorine leading to a mass gain and the volatilization of the main gaseous product, aluminium chloride, with a mass loss of the sample. These processes take place simultaneously during the course of the reaction. A kinetic model is proposed to describe these two steps providing a simple method for linearization of the initial part of the isothermal TG curves. Temperature and partial pressure dependence of the reaction rate and of the steady-state surface coverage are discussed on the basis of the proposed kinetic model. Activation energies and reaction orders are calculated for these two steps.

INTRODUCTION

Gravimetric methods are often used to study the kinetics and mechanism of heterogeneous reactions, in which the fraction of the solid reacted can be calculated from the exact determination of the mass change of the sample [1]. However, various processes associated with mass gain, like chemisorption, and with mass loss, like volatilization, may occur simultaneously causing problems in the evaluation of experimental data.

In order to describe the chlorination reactions of γ-alumina thermogravimetric (TG) studies have been carried out using various reactants, e.g., CCl_4 [2,3], $COCl_2$ [3,4], $CO + Cl_2$ [3,5]. As detected earlier [2,3], during the reaction of γ-alumina with CCl_4, the substitution of the surface oxygens by chlorine and the volatilization of aluminium chloride proceed simultaneously. The present paper outlines a kinetic model for describing these two main processes.

0040-6031/84/$03.00

EXPERIMENTAL

Isothermal TG measurements were carried out in a fused silica reactor coupled with a Mettler semimicro recording balance, as described earlier [3]. In the experiments one-piece cylindrical extrusions of high purity γ-alumina (CK-300 type, produced by Ketjen, The Netherlands, with impurity level of 90 ppm SiO_2, 100 ppm Fe_2O_3, 10 ppm Na_2O) were used. Samples of 15–20 mg mass (1.6 mm diameter, 5–10 mm length) were preheated at 1023 K for 30 min in order to achieve a standard state with a low residual OH content. Typical BET specific surface area of the preheated samples was about 160 $m^2\ g^{-1}$ determined by N_2 adsorption at 77 K. Reagent grade CCl_4 (Merck) was introduced by a 4 N purity N_2 or He stream from a bubbler. The partial pressure was regulated by the temperature of the bubbler. A total inlet flow rate of 40 $cm^3\ min^{-1}$ (STP) resulted in a local linear flow rate of 16 cm min^{-1} (STP) in the reactor near to the surface of the reacting samples. Chlorination measurements were carried out in the temperature range 650–1123 K mainly at 2.1 kPa CCl_4 partial pressure. The influence of the CCl_4 pressure was studied in the range 10^2–10^4 Pa CCl_4.

KINETIC MODEL FOR THE CHLORINATION PROCESS

As previously shown [2], in the temperature range 650–1123 K, all of the isothermal curves start with a weight gain, developing immediately after the introduction of CCl_4. This stage is followed by a steady-state mass loss which changes to a deceleratory curve at higher conversions. A typical isothermal mass change vs. time curve demonstrating this behaviour is shown in Fig. 1. In another isothermal measurement (Fig. 2) the flow of the active gas was interrupted several times. As anticipated, the volatilization

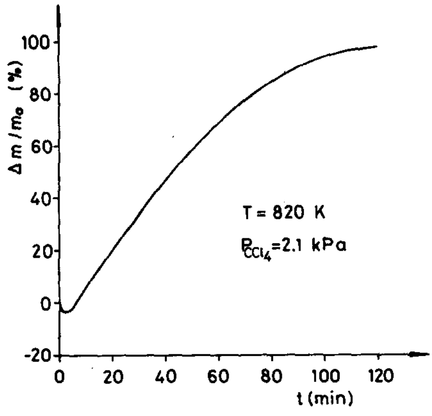

Fig. 1. A typical isothermal mass loss vs. time plot ($T = 820$ K, $p = 2.1$ kPa CCl_4).

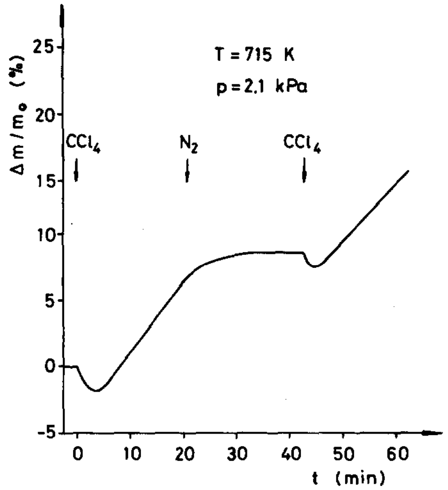

Fig. 2. The effect of the interruption of the CCl_4 stream on the isothermal TG curve during the course of the reaction ($T = 715$ K, $p = 2.1$ kPa CCl_4).

rate decreases in the inert atmosphere and asymptotically approaches zero. The repeated introduction of CCl_4 causes a further, but smaller, mass gain. This observation leads to the conclusion that the mass gain observed at the beginning of the chlorination process is caused by the formation of a certain amount of surface coverage which is in dynamic interaction with the gas phase, and that the chlorination reaction takes place in two main steps: first, some of the surface oxygen atoms are substituted by chlorine atoms; and later, these surface species react with CCl_4 resulting in the volatilization of aluminium chloride. The structure of the surface can be described by eqn. (1) from Basset et al. [6,7]

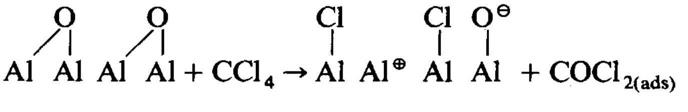

$$\mathrm{Al\ \overset{O}{Al}\ Al\ \overset{O}{Al} + CCl_4 \rightarrow \overset{Cl}{Al}\ Al^{\oplus}\ \overset{Cl}{Al}\ \overset{O^{\ominus}}{Al} + COCl_{2(ads)}} \qquad (1)$$

Aluminium chloride is assumed to form either by the reaction between the substituted surface species and the CCl_4, or by a surface rearrangement. During the chlorination reaction adsorbed $COCl_2$ is formed which may further react as chlorinating agent or may desorb from the surface, depending on the experimental conditions.

The substitution and the volatilization processes are simultaneous during the course of the reaction but contribute oppositely to the mass change (see Fig. 3).

Thus, the measured mass change of the sample (curve a, Fig. 3) consists of a mass gain (curve b, Fig. 3), caused by the formation of surface coverage, and a mass loss (curve c, Fig. 3) due to the gasification process. At the

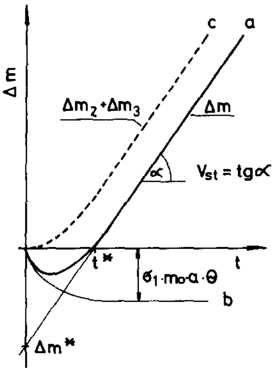

Fig. 3. The initial part of the isothermal TG curve.

beginning of the chlorination process the surface coverage can be described by the following simplified equation

$$\dot{\theta} = k_1(1-\theta) - (k_2 + k_3)\theta \tag{2}$$

where k_i is the apparent rate constant of the appropriate process: namely the oxygen substitution by chlorine (k_1); the volatilization of aluminium chloride from this substituted surface due to the reaction between the surface species and CCl_4 (k_2); and without CCl_4 by a surface rearrangement (k_3). The rate constants include their pressure dependence term, described by the formal reaction orders n and m in the case of chlorine substitution (k_1) and the reaction between the surface species and CCl_4 (k_2), respectively. The temperature dependence of the apparent rate constants is assumed to obey an Arrhenius type law

$$k_1 = k_1^0\,\mathrm{e}^{-E_1/RT}p^n \tag{3}$$

$$k_2 = k_2^0\,\mathrm{e}^{-E_2/RT}p^m \tag{4}$$

$$k_3 = k_3^0\,\mathrm{e}^{-E_3/RT} \tag{5}$$

The integral form of eqn. (2) is

$$\int_0^\theta \frac{\mathrm{d}\theta}{k_1 - (k_1 + k_2 + k_3)\theta} = \int_0^t \mathrm{d}t \tag{6}$$

By solving eqn. (6) we obtain the expression for the chemisorption coverage

$$\theta = (k_1/A)(1 - \mathrm{e}^{-At}) \tag{7}$$

where $A = k_1 + k_2 + k_3$.

From eqn. (7) the steady-state coverage can be expressed as

$$\theta_{st} = k_1/A = k_1/(k_1 + k_2 + k_3) \tag{8}$$

The change in sample weight consists of a mass gain, which is proportional to the actual surface coverage, and a mass loss caused by the volatilization of the aluminium chloride product (Fig. 3).

The latter can be formed by the reaction between the surface species and $CCl_4(\Delta m_2)$ or by the rearrangement of the substituted surface (Δm_3)

$$\Delta m = -\sigma_1 m_0 a\theta + \Delta m_2 + \Delta m_3 \tag{9}$$

where m_0 is the initial sample mass (mg), a is the specific surface area of the sample (m^2 mg^{-1}) and σ_1 is a factor characterizing the surface oxygen substitution by chlorine (mg m^{-2}). The value of σ_1 can be calculated on the basis of eqn. (1) with the knowledge of the area occupied by an oxygen ion in the (100) plane of the cubic, close packed oxide lattice in the case of an ideal dry γ-alumina surface [8].

The volatilization rate of the chloride product is proportional, in both cases, to an apparent rate constant and to the surface coverage, and can be described as

$$\dot{m}_2 = \sigma_2 m_0 a k_2 \theta \tag{10}$$

$$\dot{m}_3 = \sigma_3 m_0 a k_3 \theta \tag{11}$$

where σ_2 and σ_3 are factors (mg m^{-2}) characterizing the volatilization process with and without CCl_4, respectively, and can be calculated with the knowledge of the stoichiometric relations of the aluminium chloride formation due to the reaction of the surface species by CCl_4 and due to the surface rearrangement. Solving eqns. (10) and (11) Δm_2 and Δm_3 may be determined and replaced in eqn. (9). In this way a relationship can be obtained between the mass change of the sample and the reaction time

$$\Delta m = -m_0 a\theta_{st}\left(\sigma_1 + \sigma_2\frac{k_2}{A} + \sigma_3\frac{k_3}{A}\right)(1 - e^{-At}) + m_0 a\theta_{st}(\sigma_2 k_2 + \sigma_3 k_3)t \tag{12}$$

Three parameters characterizing the isothermal TG curve can be derived from eqn. (12).

(1) The slope of the linear part of the isothermal TG curve, i.e., steady-state reaction rate

$$v_{st} = m_0 a\theta_{st}(\sigma_2 k_2 + \sigma_3 k_3) \tag{13}$$

(2) The intercept (Δm^*) obtained by extending the quasi-linear part of the isothermal TG curve, defined above as v_{st}, back to the mass change axis

$$\Delta m^* = m_0 a\theta_{st}\left(\sigma_1 + \sigma_2\frac{k_2}{A} + \sigma_3\frac{k_3}{A}\right) \tag{14}$$

(3) The intercept of the above defined linear part of the isothermal TG curve to the time axis (termed as time intercept, t^*) is

$$t^* = \sigma_1/(\sigma_2 k_2 + \sigma_3 k_3) + 1/A \tag{15}$$

The mass loss vs. time curves can be rewritten in the function of the above parameters as follows

$$\Delta m = -\Delta m^*(1 - e^{-At}) + v_{st}t \tag{16}$$

Rearranging and taking logs, eqn. (16) becomes

$$-At = \ln[1 + (\Delta m - v_{st}t)/\Delta m^*] \tag{17}$$

Thus, the plot of $\ln[1 + (\Delta m - v_{st}t)/\Delta m^*]$ vs. t will give a straight line.

It is worthwhile to investigate the generalized eqns. (13), (14) and (15) under four particular conditions as shown in Table 1. First, consider that when the exchange reaction is much faster than the volatilization process (cases Ia and Ib) the surface is nearly completely covered by chlorine. The intercept is nearly equal to the mass gain caused by the surface coverage. The steady-state reaction rate and the time intercept are controlled by k_2 in Ia and by k_3 in Ib. In IIa and IIb the coverage is low due to the fast gasification of aluminium chloride and is controlled by the ratio of the apparent rate constants of the substitution (k_1) and of the volatilization (k_2, k_3) processes. The steady-state reaction rate is determined by k_1 while the time intercept is controlled by the volatilization processes.

As can be seen in Fig. 2 the reaction rate decreases rapidly to zero after stopping the flow of CCl_4. Considering this observation it may be assumed that k_3 can be neglected in comparison with $(k_1 + k_2)$.

In this case, from eqn. (8)

$$\theta_{st} = k_1/(k_1 + k_2) \tag{18}$$

$$k_2/(k_1 + k_2) = 1 - \theta_{st} \tag{19}$$

and from eqn. (14)

$$\Delta m^* = m_0 a \theta_{st}[\sigma_1 + \sigma_2(1 - \theta_{st})] \tag{20}$$

TABLE 1

Particular cases derived from eqns. (13), (14) and (15)

Particular conditions	Case I ($k_1 \gg k_2 + k_3$)		Case II ($k_1 \ll k_2 + k_3$)	
	Ia($\sigma_2 k_2 \gg \sigma_3 k_3$)	Ib($\sigma_2 k_2 \ll \sigma_3 k_3$)	IIa($\sigma_2 k_2 \gg \sigma_3 k_3$)	IIb($\sigma_2 k_2 \ll \sigma_3 k_3$)
Steady-state coverage (θ_{st})	1	1	k_1/k_2	k_1/k_3
Intercept (Δm^*)	$\sigma_1 m_0 a$	$\sigma_1 m_0 a$	$(\sigma_1 + \sigma_2) m_0 a \theta_{st}$	$(\sigma_1 + \sigma_3) m_0 a \theta_{st}$
Steady-state reaction rate (v_{st})	$\sigma_2 m_0 a k_2$	$\sigma_3 m_0 a k_3$	$\sigma_2 m_0 a k_1$	$\sigma_3 m_0 a k_1$
Time intercept (t^*)	$\sigma_1/\sigma_2 k_2$	$\sigma_1/\sigma_3 k_3$	$(\sigma_1 + \sigma_2)/\sigma_2 k_2$	$(\sigma_1 + \sigma_3)/\sigma_1 k_3$

In that case the steady state coverage can be expressed as

$$\theta_{\mathrm{st}} = \frac{\sigma_1 + \sigma_2}{2\sigma_1} \pm \left[\frac{(\sigma_1 + \sigma_2)^2}{4\sigma_1^2} - \frac{\Delta m^*}{\sigma_2 m_0 a} \right]^{1/2} \tag{21}$$

At the beginning of the chlorination process the reaction rate is determined mainly by the change in the surface coverage. After the steady-state coverage has been developed the reaction rate becomes constant. Naturally, at a later stage the observed rate of the mass change decreases due to the reduction in the sample weight. It is usually assumed that the rate of an isothermal process can be described by the following equations

$$\frac{\mathrm{d}\alpha}{\mathrm{d}t} = k\mathrm{f}(\alpha) \tag{22}$$

$$\mathrm{g}(\alpha) = \frac{\mathrm{d}\alpha}{\mathrm{f}(\alpha)} = k\,\mathrm{d}t \tag{23}$$

Where α is the fraction reacted (conversion), g and f are specific functions. During the chlorination reaction the measured conversion differs slightly from the actual one by the mass gain caused by the oxygen-to-chlorine exchange. It can be deduced that when plotting the appropriate $\mathrm{g}(\alpha)$ vs. t function the slope of the straight line corresponds to the rate of the aluminium chloride formation. However, in the $\mathrm{g}(\alpha)$ vs. t representation the straight lines do not have a zero intercept because the rate equation has to be integrated with the boundary condition of $\alpha = 0$ at $t = t_0$. Thus, the curves intercept the time axis at that point, when the mass loss caused by the volatilization of aluminium chloride equals the mass gain due to the oxygen substitution by chlorine.

RESULTS AND DISCUSSION

Equation (17) provides a simple method for the linearization of the initial part of the isothermal TG curves. Fitting the mass loss vs. time curve to the proposed kinetic model the experimental data fall on a straight line. As an example for the linearization, the initial part of an experimental curve can be seen in Fig. 4a, while the logarithmic relation is represented in Fig. 4b. Correlation coefficients of 0.995–0.999 were obtained for the transient range $0 \leqslant -(\Delta m - v_{\mathrm{st}}t)/\Delta m^* \leqslant 0.85$. Thus, eqn. (12) can be applied to describe the weight change vs. time curves at the beginning of the chlorination process. As demonstrated earlier [2] in the conversion range $0.10 \leqslant \alpha \leqslant 0.80$ the contracting-cylinder model proved to be the most satisfactory for describing the time dependence of the reaction rate at temperatures above 730 K in the steady-state region. The temperature dependence of the intercept is shown in Fig. 5. Δm^* increases with temperature up to 820 K, then decreases to become constant above 990 K.

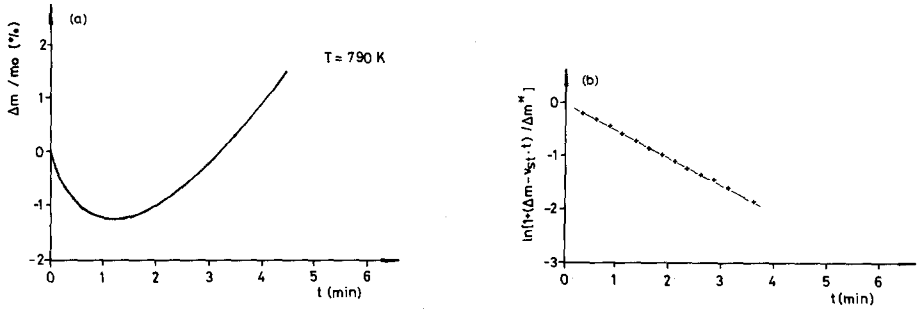

Fig. 4. An example of the linearization of the initial part of the isothermal TG curve.

Experimental results shown in Fig. 6 indicate that Δm^* is independent of the partial pressure of the active gas. The $g(\alpha)-t$ representations for the contracting-cylinder model are shown in Fig. 6. As can be seen, these lines intercept the $g(\alpha)$ axis at the same point for various partial pressures and different positions of the sample. Moreover, the same intercept is obtained for powder-like samples as well as cylindrical extrusions. While the slope of the plots, and, accordingly, the reaction rate is different in these cases, the intercept does not depend on the partial pressure of the active gas and on the above experimental conditions, which affect, however, the gas concentration in the vicinity of the sample. As can be seen from Table 1 while in case I Δm^* is constant, in case II the intercept is independent of the CCl_4 concentration only in cases when the same reaction order can be applied to describe the substitution and the volatilization processes ($n = m$).

On the basis of the temperature and pressure dependence of Δm^* the ratio of the rate constants (k_1/k_2) can be estimated. Below 820 K the intercept increases with temperature, but is independent of the partial pressure of CCl_4, consequently the oxygen substitution by chlorine is slow compared to the rate of the volatilization step ($k_1 < k_2$). Above 990 K the temperature and the partial pressure do not affect the intercept, thus the slowest process is the gasification of the chloride product ($k_1 > k_2$). Below

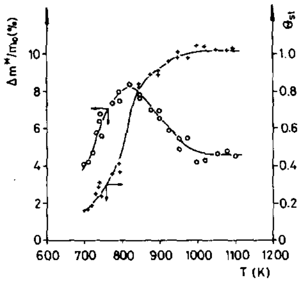

Fig. 5. The temperature dependence of the intercept ($p_{CCl_4} = 2.1$ kPa) measured and of the steady-state coverage calculated from eqn. (20).

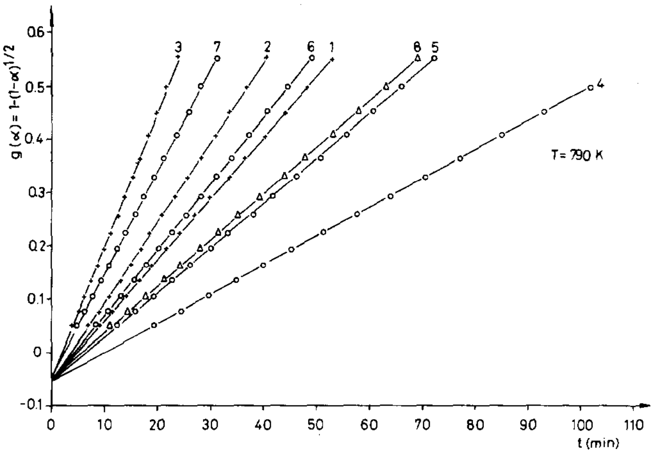

Fig. 6. $g(\alpha)-t$ representations for the chlorination of γ-Al_2O_3 by CCl_4 made under various experimental conditions, $T = 790$ K. (1) 2.1 kPa; (2) 3.2 kPa; (3) 6.9 kPa; (4) 1.6 kPa; (5) 2.1 kPa; (6) 4.2 kPa; (7) 9.1 kPa; (8) 2.1 kPa; (+) cylindrical sample, supported by a twin-armed fused silica hanger; (○) cylindrical sample in fused silica crucible; (△) powder sample in fused silica crucible.

820 K, therefore, the temperature dependence of v_{st} is determined by the activation energies of oxygen substitution by chlorine (k_1), while the t^* value is controlled by the volatilization step (k_2; Table 1).

The Arrhenius representation of the reaction rate and the time intercept is shown in Fig. 7. Two different activation energies were obtained in two temperature ranges in both cases. From the slopes of the Arrhenius plots values of 209 and 105 kJ mol^{-1} were calculated for the oxygen substitution by chlorine in the temperature ranges 650–720 and 720–820 K, while 163 and 81 kJ mol^{-1} were obtained for the volatilization process for the same temperature ranges (Table 2). Below 720 K the reaction takes place in the chemical control region as demonstrated earlier [2]. Above 720 K transport

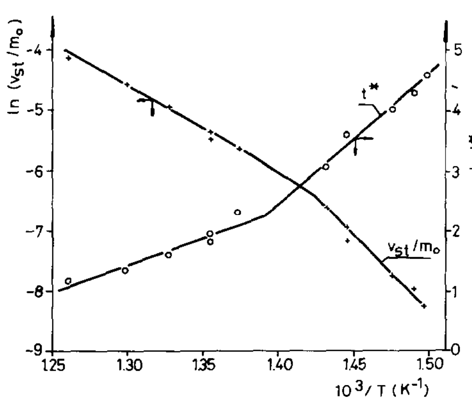

Fig. 7. Arrhenius representation of the reaction rate and of time intercept.

TABLE 2

Activation energies and reaction orders for the chlorination process

	n, m	E_1 (kJ mol^{-1})	E_2 (kJ mol^{-1})
Temperature dependence			
650–720 K	–	209	163
720–820 K	–	105	81
Pressure dependence			
700–720 K	0.5	–	–
720–820 K	0.75	110	89

processes affect the reaction rate. The apparent activation energy calculated for these higher temperatures is about half the value obtained in the chemical control region. It is interesting to note that the steady-state coverage (and also the intercept) is independent of the rate of pore diffusion because it is independent of the partial pressure of the active gas. This conclusion is in good agreement with the observation that the surface coverage causes a measurable weight gain at the beginning of the chlorination reaction even at higher temperatures, when the chlorination is determined by the mass transfer and the reaction takes place on the external surface of the sample. Detailed discussion of the influence of the transport processes will be given in the second part of this work [9].

Chlorination measurements were carried out in the partial pressure range 10^3–10^4 Pa CCl_4. Studying the influence of the CCl_4 concentration on v_{st} and t^*, a reaction order of 0.5 and 0.75 was obtained below and above 720 K, respectively, for both the substitution and the volatilization steps. As a consequence, linear plots were obtained by representing the $v_{st} - p^{1/2}$ and $t^* - p^{-1/2}$ functions below 720 K while the functions $v_{st} - p^{3/4}$ and $t^* - p^{-3/4}$ gave straight lines at higher temperatures (Figs. 8–11).

The $\sqrt{p}$ dependence of the reaction rate can be explained by a fast

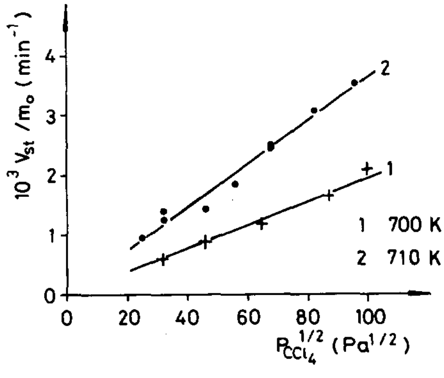

Fig. 8. Plots of v_{st}/m_0 vs. $p^{1/2}$.

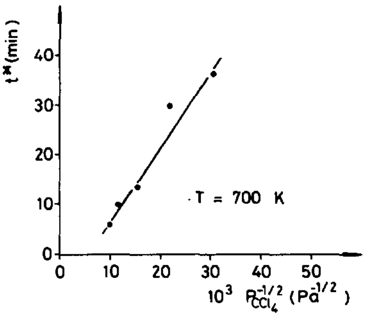

Fig. 9. Plot of t^* vs. $p^{-1/2}$.

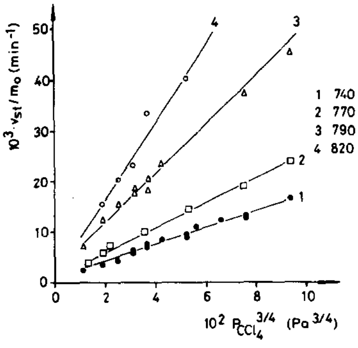

Fig. 10. Plots of v_{st}/m_0 vs. $p^{3/4}$.

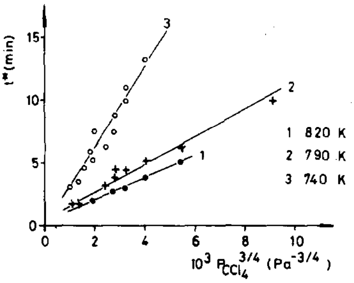

Fig. 11. Plots of t^* vs. $p^{-3/4}$.

dissociative adsorption of CCl_4 on the alumina surface. Similar to the interpretation of the $V_2O_5 + CCl_4$ reaction [10] a mechanism based on the rapid and reversible formation of $Cl^{\cdot}$ and $CCl_3^{\cdot}$ radicals may also be suggested for the present case. In the substitution step $Cl^{\cdot}$ and $CCl_3^{\cdot}$ radicals react with the alumina surface resulting in the oxygen–chlorine exchange and this dissociative adsorption equilibrium also precedes the volatilization process.

Rate constants were calculated from the partial-pressure dependence of v_{st} and t^*. In the temperature range 720–820 K the apparent activation energies $E_1 = 110$ and $E_2 = 89$ kJ mol^{-1}, obtained for the substitution and for the volatilization processes (Table 2), are in good agreement with the values calculated from the temperature dependence.

The steady-state coverage can be calculated from eqn. (20) knowing the values of Δm^*, the factors $\sigma_1 (= 0.29$ mg m$^{-2})$ and $\sigma_2 (= 1.35$ mg m$^{-2})$, and the specific surface area (0.16 m^2 mg^{-1}). The temperature dependence of the calculated surface coverage is shown in Fig. 5. θ_{st} starts at a relatively low value increasing up to the completely covered surface with increasing temperature. This is because the apparent activation energy of chlorine substitution is larger than that of the volatilization process ($E_1 > E_2$). At low temperatures the intercept can be expressed by the equation $\Delta m^*/m_0 = (\sigma_1 + \sigma_2)\ ak_1/k_2$. Above 820 K, however, k_1 cannot be neglected in the denominator, and so this equation cannot be applied. At higher temperatures $k_1 \gg k_2 + k_3$, $\theta_{st} \approx 1$ and $\Delta m^*/m_0 \simeq \sigma_1 a$ will be valid. Thus, above 820 K, the ratio of k_1/k_2 and the steady-state coverage increases with increasing temperature, however, there is a reduction in the intercept. After forming $\theta_{st} \approx 1$ the Δm^* will be independent of the temperature. Above 990 K the measured intercepts are about 0.05, which is equal to the value calculated from the completely covered surface, i.e., $\sigma_1 a = 0.046$.

CONCLUSIONS

The chlorination reaction under study takes place in two steps. At first some of the surface oxygen atoms are substituted by chlorine atoms. These surface species react with CCl_4, resulting in the volatilization of the chloride product. The oxygen substitution by chlorine on the surface and the volatilization of the gaseous products are simultaneous. On the basis of the proposed model, relationships were obtained between the parameters characterizing the TG curves and the reaction rates corresponding to the two steps.

The model provides a simple method for linearization of the initial part of the isothermal TG curves. Experimental results indicate that the overall rate is controlled by the substitution step at low temperatures ($T < 820$ K) and by the volatilization process at high temperatures ($T < 990$ K). The steady-state coverage increases with temperature up to the nearly completely covered surface; it will be constant above 990 K, and its value does not depend on the partial pressure of the active gas. In the temperature range 650–720 K activation energies of 209 and 163 kJ mol^{-1} were calculated for the substitution and the volatilization steps, respectively. Both steps can be characterized by a reaction order of 0.5 below 720 K and 0.75 above 720 K.

ACKNOWLEDGEMENTS

The authors are much indebted to Professors Gy. Varsányi and T. Székely for their valuable discussions and advice, and also to I. Lengyel for technical help in performing experiments.

LIST OF SYMBOLS

a	specific surface area (m^2 mg^{-1})
k_1, k_2, k_3	apparent rate constants
m_0	initial sample mass (mg)
Δm	mass loss of the sample (mg)
Δm_2	mass loss due to the reaction between the substituted surface and CCl_4 (mg)
Δm_3	mass loss due to the aluminium chloride desorption after a surface rearrangement (mg)
Δm^*	the intercept obtained by extending the linear part of the isothermal TG curve with the mass change axis (intercept; mg)
n, m	reaction orders
t	reaction time (min)

t^*	the intercept obtained by extending the linear part of the isothermal TG curve with the time axis (time intercept; min)
v_{st}	the slope of the linear part of the isothermal TG curve (steady-state reaction rate; mg min^{-1})
θ	coverage
θ_{st}	steady-state coverage
σ_1, σ_2, σ_3	factors (mg m^{-2})

REFERENCES

1 J. Székely, J.W. Evans and H.Y. Sohn, Gas–Solid Reactions, Academic Press, London, 1976.
2 I. Bertóti, I.S. Pap, T. Székely and A. Tóth, Thermochim. Acta, 41 (1980) 27.
3 I. Bertóti, A. Tóth, I.S. Pap and T. Székely, Thermal Analysis, ICTA 80, Vol 2, Birkhaeuser Verlag, Basel, Boston, Stuttgart, 1980, p. 235.
4 I. Bertóti, A. Tóth, T. Székely and I.S. Pap, Thermochim. Acta, 44 (1981) 325.
5 A. Tóth, I. Bertóti and T. Székely, Thermochim. Acta, 52 (1982) 211.
6 J. Basset, M.V. Mathieu and M. Prettre, J. Chim. Phys. Phys. Chim. Biol., 66 (1969) 611.
7 J. Basset, M.V. Mathieu and M. Prettre, Rev. Chim. Miner., 5 (1968) 879.
8 J.B. Peri and R.B. Hannan, J. Phys. Chem., 64 (1960) 1526.
9 I.S. Pap and I. Bertóti, Thermochim. Acta, 79 (1984) 83.
10 Gy. Mink, I. Bertóti, C. Battistoni and T. Székely, React. Kinet. Catal. Lett., in press.